Biol. Cybern. 77, 367–380 (1997)

Biological Cybernetics

Phase response characteristics of model neurons determine which patterns are expressed in a ring circuit model of gait generation

C.C. Canavier[1], R.J. Butera[2,*], R.O. Dror[2], D.A. Baxter[1], J.W. Clark[2], J.H. Byrne[1]

[1] Department of Neurobiology and Anatomy, University of Texas Medical School, PO Box 20708 Houston, TX 77225, USA
[2] Department of Electrical and Computer Engineering, Rice University, Houston, TX 77251-1892, USA

Received: 20 November 1996 / Accepted: 29 July 1997

Abstract. In order to assess the relative contributions to pattern-generation of the intrinsic properties of individual neurons and of their connectivity, we examined a ring circuit composed of four complex physiologically based oscillators. This circuit produced patterns that correspond to several quadrupedal gaits, including the walk, the bound, and the gallop. An analysis using the phase response curve (PRC) of an uncoupled oscillator accurately predicted all modes exhibited by this circuit and their phasic relationships – with the caveat that in certain parameter ranges, bistability in the individual oscillators added nongait patterns that were not amenable to PRC analysis, but further enriched the pattern-generating repertoire of the circuit. The key insights in the PRC analysis were that in a gait pattern, since all oscillators are entrained at the same frequency, the phase advance or delay caused by the action of each oscillator on its postsynaptic oscillator must be the same, and the sum of the normalized phase differences around the ring must equal to an integer. As suggested by several previous studies, our analysis showed that the capacity to exhibit a large number of patterns is inherent in the ring circuit configuration. In addition, our analysis revealed that the shape of the PRC for the individual oscillators determines which of the theoretically possible modes can be generated using these oscillators as circuit elements. PRCs that have a complex shape enable a circuit to produce a wider variety of patterns, and since complex neurons tend to have complex PRCs, enriching the repertoire of patterns exhibited by a circuit may be the function of some intrinsic neuronal complexity. Our analysis showed that gait transitions, or more generally, pattern transitions, in a ring circuit do not require rewiring the circuit or any changes in the strength of the connections. Instead, transitions can be achieved by using a control parameter, such as stimulus intensity, to sculpt the PRC so that it has the appropriate shape for the desired pattern(s). A transition can then be achieved simply by changing the value of the control parameter so that the first pattern either ceases to exist or loses stability, while a second pattern either comes into existence or gains stability. Our analysis illustrates the predictive value of PRCs in circuit analysis and can be extended to provide a design method for pattern-generating circuits.

Correspondence to: J.H. Byrne (Fax: +1-713-500-0621, e-mail: jbyrne@nba19.med.uth.tmc.edu)
* *Present address:* Mathematical Research Branch, NIDDK, National Institutes of Health, 9190 Wisconsin Avenue, Suite 350, Bethesda, MD 20814, USA

1 Introduction

A central problem in neuroscience is to determine the relative contributions of network connectivity and of intrinsic neuronal properties to the activity of neural circuits. Studies in computational neuroscience tend to fall into two categories: those that emphasize network connectivity and therefore utilize simplified point-neuron models, and those that emphasize the intrinsic biophysical properties of real neurons. The best approach depends upon which details are important to the understanding of the particular phenomenon under study. In this study, we have focused on a minimal model of quadrupedal gait generation as an example of an oscillatory network underlying a biological rhythm; however, the analytical methods developed herein generalize to any system for which the basic assumptions of phase response curve theory hold (see Sect. 3.2).

In our minimal model, the circuit controlling the movement of a single leg is represented by a single oscillator. The individual oscillators associated with each leg are responsible for the dynamics of leg movement, but this study is concerned only with inter-oscillator (hence, interlimb) coupling and coordination. Ring geometries have been utilized extensively in biophysical modeling studies (Collins and Stewart 1994), and previous studies have shown that a simple ring circuit is capable of generating gait-like patterns (Collins and Stewart 1993; Collins and Richmond 1994) provided that the two front legs (and the two hind legs) are represented by nonadjacent oscillators in the ring configuration (Fig. 1). The previous studies used simple oscillators, such as the Van der Pol oscillator, as their circuit elements, and did not produce the full range of gaits associated with quadrupeds. For example, a gallop was not observed, only the more symmetric bound, and a trot was

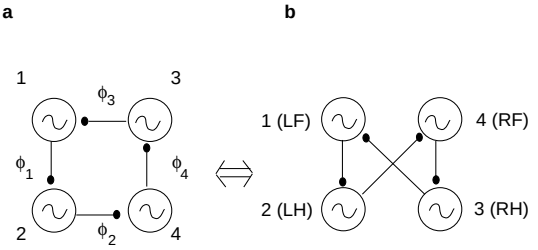

Fig. 1a,b. Network configuration. **a** Wiring diagram for the circuit: *filled circles* indicate inhibitory synapses. The phase delay between a postsynaptic oscillator and its presynaptic oscillator is denoted ϕ_i, where i refers to the presynaptic one. **b** To associate patterns of network activity with particular quadrupedal gaits, each oscillator is mapped onto a leg, either left front (LF), right front (RF), left hind (LH), or right hind (RH)

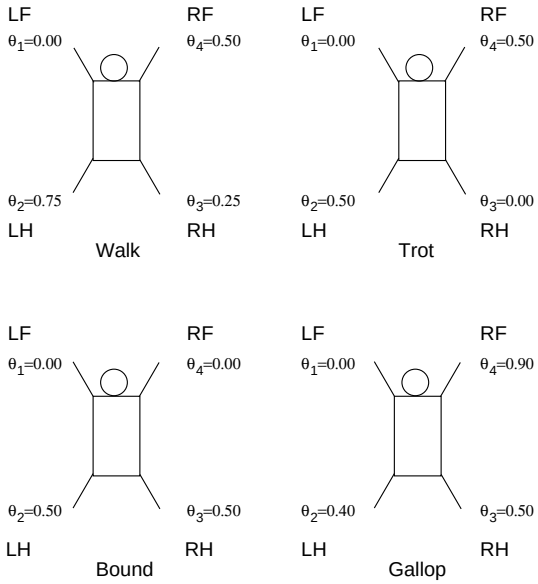

Fig. 2. Quadrupedal gaits. The stick figures may be interpreted as a quadruped viewed from above (adapted from Alexander 1984). The phasic relationships between the legs in these common gaits are indicated by the θ_i, where the phase of the LF leg was arbitrarily set to zero. For example, a θ value of 0.5 indicates that the associated leg is half a cycle, or 180^o, out of phase with the LF leg. A walk corresponds to clockwise rotation around the ring (Fig. 1), and the leg sequence LF-RH-RF-LH. In a trot, diagonal legs move together, or nearly so, and are half a cycle out of phase with the other pair. In a bound, the front legs move together, half a cycle out of phase with the hind legs. A gallop is similar to a bound, but the front legs are slightly out of phase with each other, as are the hind legs

obtained only by making the system nonautonomous due to the addition of an extrinsic sinusoidal drive. To determine whether a more complex oscillator with identical network connectivity would produce similar or qualitatively different patterns, we utilized a four variable neuronal model that captured a significant amount of the complexity of a real bursting neuron (for a complete set of equations see Butera et al. 1996).

A quadruped can move using a number of different gaits. These gaits are distinguished by both the duty cycle, which is the fraction of time a leg spends on the ground, and the phasic order of leg movement, or relative phase. This study adopts the convention of characterizing a gait by its normalized relative phases (Alexander 1984) θ_i. The relative phase for a given leg is the fraction of a step cycle, or period, by which the initiation of a step in the given (ith) leg follows that in the arbitrarily chosen reference leg. This convention assumes that each leg may be treated as a single functional unit, or oscillator (Shik and Orlovsky 1965; Grillner 1975). A quadruped typically changes gaits as its speed is increased; for example, in a cat or a horse the typical sequence as speed is increased is to proceed from a walk to a trot to a gallop.

The phasic relationships between these gaits are shown in Fig. 2, as well as the phasic relationships in a bound.[1] The walk is characterized by the sequence left front (LF), right hind (RH), right front (RF), left hind (LH), with each leg one quarter of a period out of phase with the preceding leg. In the trot, pairs of diagonal legs move in phase with each other and half a period out of phase with the other diagonal pair, whereas in the bound, the front legs move together and half a period out phase with the hind legs. The gallop is similar to the bound, but homologous contralateral legs are not exactly in phase with each other.

Other quadrupeds can exhibit numerous additional gaits (Gambaryan 1974; Hildebrand 1976, 1977), such as the pronk (or jump or gambol), in which all four legs are in phase, the lateral walk (sometimes called a reverse or backwards or diagonal walk) in which the sequence of footfalls is reversed from the more common walk, and a pace, an intermediate-speed gait like the trot in which ipsilateral legs are in phase, and in antiphase with the homologous contralateral leg (see Appendix for the relative phases of many gaits).

An important issue that this paper addresses is the nature of gait transitions. Collins (1995) identified two types of modeling studies distinguished by the manner in which gait transitions are generated: (1) by changing the relative strength (including changes to or from a synaptic weight of zero) or polarity of the couplings in a central pattern generator (CPG), thus producing different circuits in order to produce different gaits, or (2) by changing the driving signal for the CPG, thus using the same circuit to produce different gaits (see Sect. 4). Studies of spinal cats have shown that coordinated patterns of stepping can be generated at the level of the spinal cord (Halbertsma et al. 1976). Other studies have shown that the patterns can be activated or modulated by descending influences from the mesencephalic locomotor region (Shik et al. 1966; Shik and Orlovsky 1976) in fact, the application of increasingly higher levels of current to this region induces gait changes in a cat on a treadmill from a walk to a trot to a gallop. The most commonly proposed scheme for achieving gait transitions is to change the pattern of interlimb connectivity (Stafford and Barnwell 1985; Schoner et al. 1990; Yuasa and Ito 1990); the underlying assumption is that the tonic and phasic input from the central nervous system (CNS) and/or from sensory feedback modulates the weights of the connections between limbs. Another approach (Collins and Richmond 1994) is that the tonic and phasic input itself, either from the CNS or from sensory feedback, is sufficient to induce transitions without any accompanying weight changes. Although the physiological basis of gait transitions remains to be determined experimentally,

[1] Several authors have idealized the gallop as a bound (Stafford and Barnwell 1985; Schoner et al. 1990; Collins and Richmond 1994), but we have treated them as separate gaits.

we will show that neither changes in interlimb coordination nor changes in phasic input are required, but that changes in tonic input alone could be sufficient to cause observed gait transitions if the individual oscillators associated with each leg have the appropriate phase response characteristics.

In this study, the constant, nonoscillatory input to the individual oscillators is represented by I_{STIM}, the external stimulus current; all oscillators receive the same external stimulus current. I_{STIM} is a key parameter in the model of the uncoupled oscillator because it can drive its activity from hyperpolarized silence at sufficiently negative values, to bursting at an intermediate range of values, to tonic depolarization, or beating, at the most depolarized values (Fig. 3). In a physiological sense, an increase in I_{STIM} could be interpreted as an increase in the intensity of the stimulation of the CPG from higher centers, such as when an animal desires to increase its speed. Alternatively, an increase in I_{STIM} could be interpreted as an increase in intensity of some sensory feedback signal, such as that which might be received by the CPG with increased speed of a treadmill on which an animal is stepping.

Previous studies have shown that complexity manifested as the capacity to generate multiple patterns of activity is inherent in the ring pattern of connectivity (Collins and Stewart 1993, 1994; Collins and Richmond 1994). In the present study, we incorporate additional complexity in the form of physiologically-based intrinsic complexity of the circuit elements (see Sect. 2). Yet another source of complexity in our model is that the individual oscillators are bistable for a range of values of I_{STIM}. Specifically, at constant parameter values (including that of I_{STIM}), an individual oscillator can display either tonically depolarized activity in which the average spike frequency is always above zero, or bursting activity in which the spike frequency exceeds zero during bursts but is zero in the hyperpolarized interval between bursts. In order to understand and predict some of the oscillatory modes that can be generated in a ring configuration, we employed phase response curves, also known as phase-resetting curves.

2 Methods

The circuit simulator was written in C but employed a fifth-order, implicit, variable step size Runge-Kutta method subroutine (Hairer and Wanner 1991) written in Fortran. The simulations were compiled and run on both Sun Sparc2 and Sparc20 Unix workstations. The model that we employed is referred to by Butera et al. (1996) as the reduced model, and it has four state variables: membrane potential (V), intracellular calcium concentration (c), average spike frequency (q), and the activation (s) of the current that is the key determinant of bursting activity. Although the model does not produce discrete spikes, the average spike frequency q is a function of the other three variables. Moreover, the rates of change of s and c are in turn dependent on q. This feedback effect enhances the complexity of the response of the oscillator to changes in inputs. The equations and parameters for each of the four individual oscillators are identical to those given by Butera et al. (1996) for their reduced model, except that terms that depend implicitly or explicitly on the total current were modified[2] to include the synaptic current that coupled the oscillators:

$$I_{SYN}(V, q_{PRE}) = \begin{cases} g_{SYN}\ q_{PRE}(V - E_{SYN}) & \text{if } q_{PRE} \geq 0 \\ 0 & \text{otherwise} \end{cases}$$

where the synaptic strength g_{SYN} was set to 0.001 μS/Hz, q_{PRE} is the spike frequency (Hz) in the presynaptic neuron, V is the membrane potential in the postsynaptic neuron, and the reversal potential E_{SYN} for the synaptic current was set to -70 mV to produce inhibitory connections. The units for g_{SYN} are in μS/Hz because the synaptic current in the postsynaptic neuron is a function of the spike frequency of the presynaptic neuron. The value for g_{SYN} was heuristically determined by setting it to a value high enough to allow the circuit to become entrained within a reasonable period of time but not so high as to produce perturbations in membrane potential of the same order of magnitude as the oscillation. At this value, numerous cycles may be required to obtain phase-locked entrainment in many of the modes identified. Entrainment occurs more quickly if the synaptic weights are increased tenfold, but some of the interesting modes disappear. Since the same principles of circuit analysis apply in either case, the conductance was set at this low value for illustrative purposes. Since the modulatory effects of serotonin (5-HT) and dopamine (DA) were not considered, the concentrations [5-HT] and [DA] were set to zero; I_{STIM} was varied as noted in the text and figure legends. The output of the individual oscillators associated with each leg (Fig. 1) was interpreted as only providing the timing for the initiation of leg movement, which was assumed to coincide with burst initiation in the corresponding oscillator. A burst is initiated when the average spike frequency q becomes greater than zero, and terminated when it falls below zero. Figure 3 illustrates the output of an individual oscillator that corresponds to silent hyperpolarized, bursting, and beating electrical activity.

3 Results

3.1 Random search of state space

To determine the possible modes exhibited by this circuit, two methods were employed. The first was random and empirical, whereas the second approach had a theoretical component. In the first method, the intent was to determine, in an approximate way, the fraction of the relevant state space occupied by the attractor associated with each mode, based on the frequency of occurrence of each mode in a series of random trials. The underlying assumption was that a nonlinear system of this complexity would contain multiple attractors in its state space even at constant parameter settings (Guckenheimer and Holmes 1983; Goldbeter 1996). We therefore

[2] These are the modified equations (the terms are explained in Butera et al. 1996):

$$\begin{aligned} I_{sub}(V, c, s, q_{pre}) &= I_{SI}(V, c, s) + I_R(V) + I_L(V) + I_{NaCa}(V, c) \\ &\quad + I_{CaP}(c) + I_{NaK}(V) + I_{SYN}(V, q_{PRE}) \\ m_L &= N_R(C_{cAMP})[m_{L0} + (I_{SYN} - I_{STIM})/2.0] \\ b_L &= [b_{L0} + (I_{SYN} - I_{STIM})/25.0]/N_R(C_{cAMP})\ . \end{aligned}$$

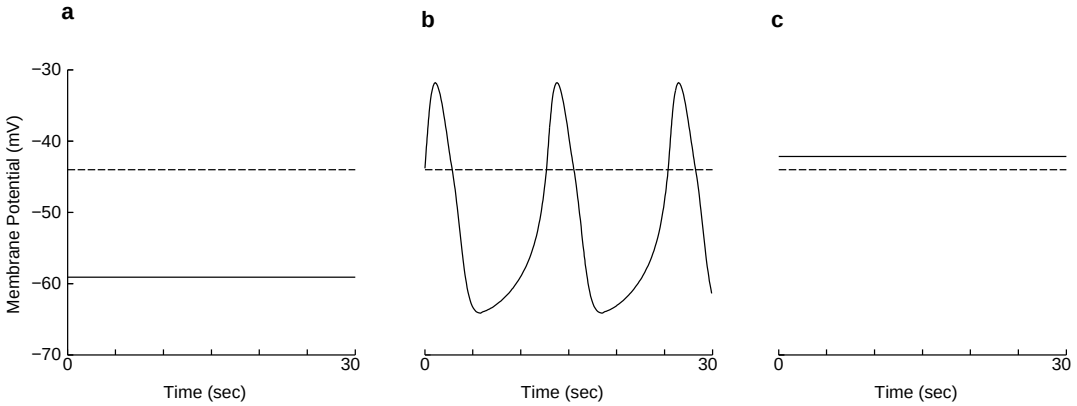

Fig. 3a–c. Output of an uncoupled oscillator as I_{STIM} is varied. The dashed line indicates the approximate spike threshold; above this line average spike frequency q is greater than zero. **a** At hyperpolarizing values of I_{STIM} (-0.6 nA), the model neuron is silent because membrane potential never exceeds the spike threshold; q is always less than zero. A negative value of q (not shown) is interpreted as a spike frequency of zero. **b** With no extrinsic stimulus current, bursting activity is exhibited. During bursting activity, the spike frequency exceeds zero during bursts but is zero in the hyperpolarized interval between bursts. **c** At depolarizing values of I_{STIM} (2.5 nA), beating activity is observed. During tonically depolarized activity, the average spike frequency is always above zero

determined the approximate range for each state variable (V, s, c, q) during a typical oscillation, and prepared randomized sets of initial conditions for all four oscillators (16 initial conditions required for each run). This method is necessarily approximate because it is difficult to determine how to sample the state space so as not to miss any attractors. As a compromise between a reasonably large number of points and a reasonable amount of simulation time, simulations using the same set of 256 initial conditions were run at several values of I_{STIM}.

The results of the simulations are given in Fig. 4 by the numbers in parentheses. For values of I_{STIM} much more hyperpolarized than -0.5 nA, the circuit did not oscillate, but rather remained hyperpolarized (not shown). At -0.5 nA, two curious modes were observed, which are referred to as a 'staccato' gallop (Fig. 4a1) and a 'staccato' walk (Fig. 4a2). These modes have the correct sequence of activation, but not the correct phasing, for a gallop or a walk respectively. The four possible rotational variants (only one is shown for each) of the 'staccato' modes were in all cases observed in roughly equal proportions. The staccato label indicates that the four oscillators fire sequentially, then pause before the sequence begins again. We are not aware that corresponding gaits have been reported in mammals. At higher (more depolarized) values of stimulus intensity, the phasing approaches the nominal values for the gallop (Fig. 4b1) and achieves them for the walk (Fig. 4b2). The numbers in part Fig. 4b add up to only 254 because in one case a bound was observed and in another a lateral walk was observed (not shown). At 0 nA, the gallop is no longer observed, but the bound occurred frequently and the walk persisted (Fig. 4c). The numbers in part Fig. 4c again add up to only 255 because in one case a lateral walk was observed (not shown). In summary, multiple gait-like modes of oscillation were observed at all values of I_{STIM} for which individual circuit elements oscillate (but see Sect. 3.5), and both the types of gait-like modes and their relative frequencies of occurrence changed as I_{STIM} was varied.

3.2 Phase response curve analysis

The second method that we employed to determine the possible modes exhibited by this circuit also addressed why the circuit exhibited these modes at given background levels of I_{STIM}. This method used the phase response curve (PRC) of an oscillator to predict phase-locked entrainment of that oscillator (Moore et al. 1963; Perkel et al. 1964; Pavlidis 1973; Winfree 1980; Glass and Mackey 1988; Kopell 1988; Murray 1989; Demir et al. 1997). The PRC is obtained by examining an uncoupled oscillator, applying a perturbation at a given phase in the cycle, and recording the change in the period of the cycle in which the perturbation occurs. The intrinsic period of the oscillator is P_0, and the phase of the applied stimulus is $\phi = t_s/P_0$, where t_s is the time since the beginning of the burst. The length of the cycle where the perturbation occurred is $P_1(\phi)$, since the length of the perturbed cycle is a function of the phase of the stimulus application. The normalized PRC is represented by $F(\phi)$, where $F(\phi) = (P_1(\phi) - P_0)/P_0$, so that a positive value represents a phase delay and a negative value a phase advance.

In the present study, the PRC was obtained by using a perturbation generated by a single burst from an identical neuron acting at a synapse identical to the ones used in the circuit (Fig. 5). Specifically, the postsynaptic neuron was initialized at the beginning of a burst and the presynaptic neuron was also intialized at the beginning of a burst but at a phase $\phi = t_s/P_0$. Here, ϕ is the normalized difference in phase between the presynaptic and postsynaptic oscillators (normalized by the intrinsic period). Then the perturbed period P_1 was measured, and the protocol was repeated as t_s was varied through a range of values corresponding to ϕ between 0 and 1. This form for the perturbation was chosen to simulate as closely as possible the input that an oscillator receives when it is a component of a ring circuit, provided that the entrained frequency is not too different from the intrinsic frequency. Traditionally, PRC analyses have used short perturbations. Since we use perturbations that last for a significant fraction of the burst cycle, it is possible that a perturbation given late in the cycle will affect the timing not

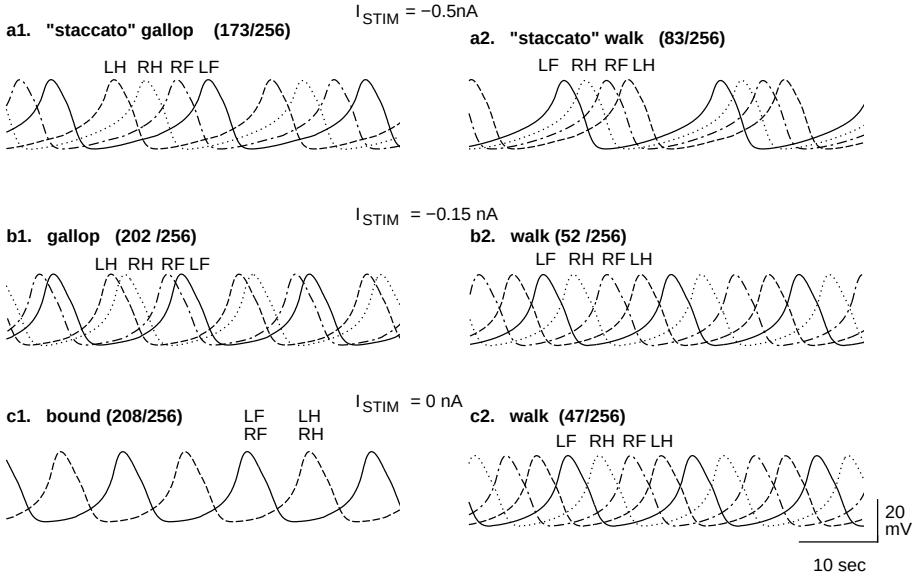

Fig. 4a–c. Oscillatory patterns as a result of a random search as I_{STIM} is varied. The numbers in *parentheses* indicate the number of stimulations that produced the corresponding mode of oscillation at each of three constant values of I_{STIM}. The 'staccato gallop' (**a1**) and the 'staccato walk' (**a2**) are so called because each sequence of steps is punctuated by a pause. As the stimulus intensity was increased, the gallop developed approximately correct phasing (**b1**), as did the walk (**b2**). A further increase in stimulus intensity caused the bound to replace the gallop (**c1**), whereas the walk remained (**c2**)

only of the cycle in which it is given, but also of the next one (Fig. 6), if the cycle is defined as the period between burst initiations. The assumption (described below) that the perturbation only affects a single cycle can be retained if the cycle is measured, as shown in Fig. 6, from the time the perturbation is applied until the same point in the cycle is reached again. In practice, it is simpler and still sufficiently accurate to determine the change in cycle length by measuring the time of occurrence of the second burst after the perturbation (P_2), then subtracting an unperturbed period to obtain P_1. Hence, we adopted this protocol: ($P_2 - P_0 = P_1$).

Our predictions of gait modes are based on the following assumptions. First, we assume that the PRC is sufficient to completely describe the dynamics of the oscillator. In other words, we assume that the effects of a perturbation can be completely described as a shift in the state variables of the oscillator from one point on the limit cycle to another. This assumption is approximately valid if the system trajectory relaxes nearly back to the limit cycle oscillation within one cycle after a perturbation (Kopell 1988; Demir et al. 1997). Second, we assume that all four oscillators are entrained at the same period in a given mode (stable pattern of oscillation). This assumption is made implicitly whenever phase differences between legs or between adjacent oscillators are normalized between 0 and 1, because they are normalized by the common entrained period. Consequently, the phase differences (normalized by the entrained period) between oscillators around the ring must add up to an integer, since an oscillator must be in phase with itself. Another consequence is that each cell receives exactly one perturbational input during one entrained period, which is then equivalent to the perturbed period (P_1) discussed above, except that in the generation of the PRCs, ϕ is normalized to the intrinsic period, whereas in the circuit, ϕ is normalized to the entrained period. Thus, a link can be made from the analysis of the circuit to the PRC. The phase difference between adjacent oscillators, $\phi_i = \theta_{PRE} - \theta_{POST}$ (where i is the number of the presynaptic oscillator), is equivalent to the usage of ϕ in the generation of the PRCs as described above, except that the relative phases in the PRC generation and within the circuit are normalized to different periods. Since each oscillator receives one perturbation per cycle at a phase of ϕ_i, then $P_1 = P_0(1 + F(\phi_i))$, and $F(\phi_i)$ must have the same value for each phase difference ϕ_i around the ring.[3] In other words, since all oscillators have the same intrinsic period (P_0), they must also have the same phase advance or delay $F(\phi)$ in order to be entrained with the same period (P_1). Each oscillator is effectively entrained by its presynaptic cell at a phase difference of ϕ_i. For this entrainment to be stable given a periodic drive, the PRC must have a slope between 0 and 2 at the point $(\phi_i, F(\phi_i))$ (Moore et al. 1963; Perkel et al. 1964). This result does not apply to the ring circuit directly because no single oscillator can be considered an unperturbed periodic drive. Theoretical work in progress (Dror et al. in preparation) indicates that a slope between 0 and 1 is a sufficient but not necessary condition for stable entrainment within a ring circuit, and that slopes that are all either less than 0 or than 2 guarantee that a mode will be unstable.

Given the above assumptions and an identical PRC for each oscillator in the ring, the existence of an oscillation or gait pattern is predicted for any set of n points on the PRC such that:

$$\phi_1 + \phi_2 + \ldots + \phi_n = j(1 + F(\phi_i)), j \in [0, 3] \quad (1)$$

$$F(\phi_1) = F(\phi_2) = \ldots = F(\phi_n) \quad (2)$$

where n is the number of oscillators in the ring and all ϕ_i are normalized to the intrinsic frequency. Equation (1) formalizes the first criterion for existence of a mode: that the values of ϕ around the ring must add up to an integer (j) multiplied by a correction factor of $(1 + F(\phi))$ to account for the difference between the entrained period and the intrinsic period. Equation (2) formalizes the second criterion: that $F(\phi)$ must be the same for all values of ϕ (normalized to the intrinsic frequency). The second criterion is automatically satisfied

[3] This approach can be generalized to circuits of nonidentical oscillators. For example, if all oscillators do not have the same intrinsic period P_0, then the quantity $P_0(1 + F(\phi_i))$ must be constant for all oscillators in order for them to be entrained at the same frequency.

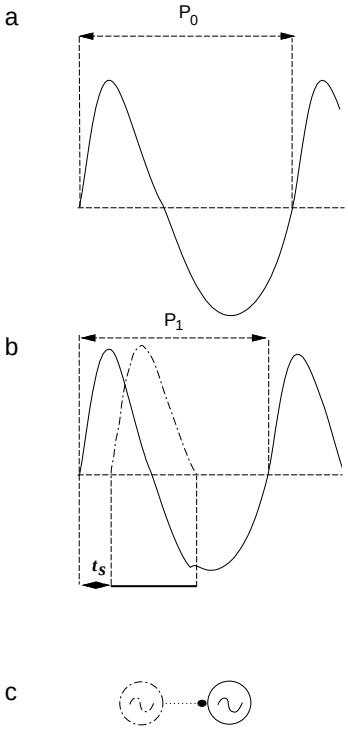

Fig. 5a–c. Method for determination of the phase response curve. **a** P_0 denotes the free-running, or intrinsic, period of the oscillator. In both **a** and **b**, the *long horizontal dashed line* indicates the voltage threshold for burst initiation, and the waveform plotted with a *continuous line* shows the variation in membrane potential for the oscillator whose PRC is being measured (indicated by a *continuous line* in part **c**). **b** P_1 denotes the perturbed period of the same oscillator. The *dot-dashed line* shows the perturbation applied at time t_s, a burst generated by the oscillator outlined by a *dot-dashed line* in part **c** The inhibitory connection shown by a *dotted line* in **c** is only enabled during the period indicated by the *horizontal bar* under the dot-dashed burst. The oscillator indicated by the *continuous line* appears to rebound from inhibition before the perturbing burst has ended; this is because the threshold for burst termination is slightly different from that for burst initiation. **c** Schematic setup for the generation of the PRC

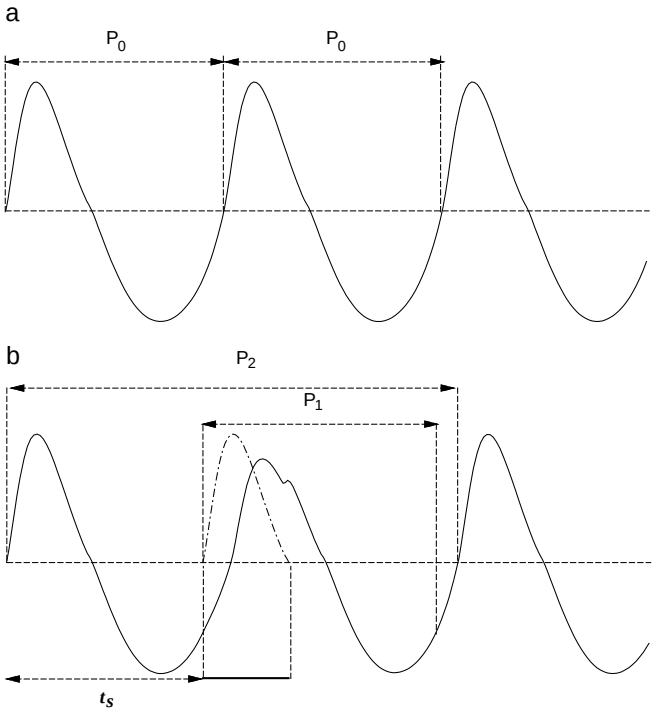

Fig. 6a,b. Long perturbations may affect the timing of two bursts. **a** Again, P_0 denotes the free-running, or intrinsic, period of the oscillator. In both **a** and **b**, the *long horizontal dashed line* indicates the voltage threshold for burst initiation, and the waveform plotted with a *continuous line* shows the variation in membrane potential for the oscillator whose PRC is being measured. **b** P_1 denotes the perturbed period of the same oscillator, and P_2 is the quantity that was measured to determine P_1. The *dot-dashed line* shows the perturbation applied at time t_s. The duration of the perturbation is shown by the *thick line*, which continues past the initiation of the first burst after the perturbation; hence it affects the timing of the second burst as well. If the perturbed cycle is defined as shown above, the assumption that only one cycle period is affected can be retained. This assumption is necessary to use the PRC to predict oscillatory modes

for the modes in which a single value of ϕ is repeated n times. We have normalized phases so that $0 \leq \phi < 1$, so there are only n distinct values of j that may give distinct solutions. In a ring circuit where n = 4, these modes correspond to the pronk (ϕ = 0, j = 0), the walk (ϕ = 0.25, j = 1, see Fig. 7a for an illustration), the bound (ϕ = 0.5, j = 2), and the lateral walk (ϕ = 0.75, j = 3), where the phases in parentheses are normalized to the entrained frequency. All possible combinations of phase differentials that meet the existence criteria for a ring circuit of four oscillators are tabulated in the Appendix. For example, all values of ϕ could be equal, or all but one equal, or there could be pairs of equal values, or all four could be distinct (the most general case). The existence of modes must be determined by examining the PRC to identify values of ϕ that satisfy the existence criteria. We implemented this scheme with a computer program that input the PRC, then determined regions of overlapping values of $F(\phi)$ and systematically searched for sets of ϕ_i that satisfied the criteria. However, existence of a mode does not guarantee that it will be observable in practice. In order to produce and detect an oscillatory mode, either in computer simulations or in the physical world, stability is required. Otherwise, the system would have to be precisely initialized and never perturbed – conditions that are impossible to achieve in practice. As mentioned above, previous work on entrained oscillators (Moore et al. 1963) and our own observations indicate that the slopes of the PRC at the points $(\phi_i, F(\phi_i))$ provide useful information regarding stability.

3.3 Phase response curve results

The PRC for an oscillator depends upon the parameters associated both with its intrinsic dynamics and with the applied perturbation (which in this study are in turn dependent upon the parameters of the synaptic coupling). Hence one would expect to have different PRCs at different values of I_{STIM}, and that the stable modes determined by the PRCs correspond to those in Fig. 4. Figure 8 illustrates how these stable modes are identified. A horizontal line indicates a fixed value of $F(\phi)$; the intersection of the horizontal line with the PRC identifies all values of ϕ for which $F(\phi)$ is identical. Then a calculation is made to determine whether there exists a set of n of these ϕ_i that satisfy (1). Parts a, b, and c in Fig. 8 show the PRCs obtained at the same values of I_{STIM} used

Table 1. Results of a search for sets of values of ϕ_i that meet the existence criteria using the three phase response curves given in Fig. 8

I_{STIM}	Gait	$1 + F(\phi)$	ϕ_1	ϕ_2	ϕ_3	ϕ_4	m_1	m_2	m_3	m_4
−0.5	pronk	1.008	0.000	0.000	0.000	0.000	−1.276	−1.276	−1.276	−1.276
−0.5	walk	0.999	0.250	0.250	0.250	0.250	−0.007	−0.007	−0.007	−0.007
−0.5	bound	0.982	0.491	0.491	0.491	0.491	−0.055	−0.055	−0.055	−0.055
−0.5	l. walk	1.096	0.822	0.822	0.822	0.822	−1.060	−1.060	−1.060	−1.060
−0.5	trot−like	0.985	0.027	0.027	0.465	0.465	−0.148	−0.148	−0.107	−0.107
−0.5	trot−like	0.996	0.144	0.144	0.354	0.354	0.158	0.158	−0.059	−0.059
−0.5	s. walk	0.999	0.188	0.270	0.270	0.270	0.024	−0.012	−0.012	−0.012
−0.5	s. walk [a]	0.995	0.136	0.136	0.136	0.587	0.167	0.167	0.167	0.345
−0.5	s. gallop[a]	0.999	0.203	0.598	0.598	0.598	0.012	0.400	0.400	0.400
−0.5	a. bound	0.990	0.417	0.417	0.573	0.573	−0.119	−0.119	0.280	0.280
−0.5	bound−like	0.983	0.476	0.476	0.476	0.537	−0.089	−0.089	−0.089	0.116
−0.5	s. l. walk	1.078	0.717	0.839	0.839	0.839	0.890	−1.066	−1.066	−1.066
−0.5	trotlike	1.038	0.669	0.669	0.887	0.887	0.725	0.725	−0.425	−0.425
−0.5	trotlike	0.988	0.013	0.094	0.440	0.440	−0.283	0.162	−0.125	−0.125
−0.5	trotlike	0.991	0.003	0.003	0.411	0.576	−0.572	−0.572	−0.113	0.293
−0.15	pronk	1.018	0.000	0.000	0.000	0.000	4.165	4.165	4.165	4.165
−0.15	walk [a]	0.997	0.249	0.249	0.249	0.249	0.027	0.027	0.027	0.027
−0.15	bound [a]	0.994	0.497	0.497	0.497	0.497	0.068	0.068	0.068	0.068
−0.15	l. walk [a]	1.040	0.780	0.780	0.780	0.780	0.068	0.068	0.068	0.068
−0.15	s. gallop	0.998	0.299	0.566	0.566	0.566	−0.003	0.104	0.104	0.104
−0.15	bound−like	0.994	0.471	0.506	0.506	0.506	−0.013	0.016	0.016	0.016
−0.15	s. l. walk	1.036	0.750	0.750	0.750	0.859	0.176	0.176	0.176	−0.255
−0.15	transitional [b]	1.020	0.000	0.680	0.680	0.680	−79.58	0.255	0.255	0.255
−0.15	transitional [b]	1.020	0.000	0.680	0.680	0.680	3.955	0.255	0.255	0.255
0.0	pronk	1.024	0.000	0.000	0.000	0.000	6.989	6.989	6.989	6.989
0.0	walk [a]	0.996	0.249	0.249	0.249	0.249	0.045	0.045	0.045	0.045
0.0	bound [a]	0.995	0.498	0.498	0.498	0.498	0.021	0.021	0.021	0.021
0.0	l. walk [a]	1.038	0.779	0.779	0.779	0.779	0.250	0.250	0.250	0.250
0.0	s. l. walk	1.035	0.750	0.750	0.750	0.860	0.155	0.155	0.155	−0.225
0.0	transitional	1.023	0.689	0.689	0.689	0.000	0.234	0.234	0.234	6.588

The m_i are the slopes of the phase responce curve (PRC) at the point $(\phi_i, F(\phi_i))$. The i designations are arbitrary: any permutation of the ϕ_i within an identified set will produce a rotational variant of the mode (see Appendix). The ϕ_i in this table are normalized to the intrinsic frequency. The predicted ϕ_i in Table 2 were obtained from the ϕ_i in this table by dividing them by $(1 + F(\phi))$, in order to predict the relative phases normalized to the entrained frequencies. Modes designated transitional are transitional between two staccato modes (see Appendix). The PRCs in this study all have a region of steep negative slope near $\phi = 0$, and in each case several modes were found with slopes more negative than −1000. These modes are predicted to be highly unstable, and were not included in this table

l., lateral; s., Staccato; a., asymmetric

[a] Modes that have only small positive slopes

[b] These modes do not differ until the fourth decimal place, so they appear identical except for the first slope

in parts a, b and c of Fig. 4, respectively. Table 1 gives the results of a systematic search for sets of ϕ_i in these PRCs that satisfy the existence criteria for oscillatory modes, as well as the slopes of the PRC at the points $(\phi_i, F(\phi_i))$. Of the sets found at $I_{STIM} = -0.5$ nA, only two had all positive slopes less than 1, and these two corresponded to the two that were observed in computer simulations (the staccato walk and staccato gallop). Similarly, at the other two values of I_{STIM}, only modes with all positive slopes were observed in the simulations, with one exception. At $I_{STIM} = -0.15$ nA, the 'gallop' was associated with a slope of −0.003. If I_{STIM} is increased any further, this mode loses its stability. This exception illustrates that while small positive slopes appear to be a sufficient condition for stability, they are not a necessary condition, as certain combinations of negative and positive slopes (but not all negative) may result in stable modes as well (Dror et al. in preparation). In addition, some modes with one or more positive slopes greater than 2 met the existence criteria but were not observed in simulations, and are probably unstable. The condition that all small positive (< 1) slopes guarantee stability has not been rigorously proven for all n, but appears to work well as a heuristic.

In Fig. 8, stable observed modes are indicated by symbols. There is a close correspondence between the phasic relationships observed during simulations and the phasic relationships predicted from the PRCs (Table 2), as well as between the entrained periods predicted by the PRCs and the observed entrained periods. Hence, the assumptions made in the PRC analysis are approximately valid. For example, in Fig. 8a, two modes are predicted: a staccato walk and a staccato gallop. In the staccato walk (the corresponding values of ϕ are indicated by circles), the PRC curve predicts that three of the four ϕ values will be equal to 0.136 and the fourth will be equal to 0.587. These values were obtained by inspecting the PRC curve (using a computer program) in Fig. 8a to determine whether any two values of ϕ with the same value of $F(\phi)$ and appropriate $F'(\phi)$ satisfied the equation $3\phi_i + \phi_j = 1(1 + F(\phi))$. The mechanics of how ϕ_i and ϕ_j that satisfy this equation result in a staccato walk are illustrated both in Fig. 7b and in the Appendix, Special Case II.

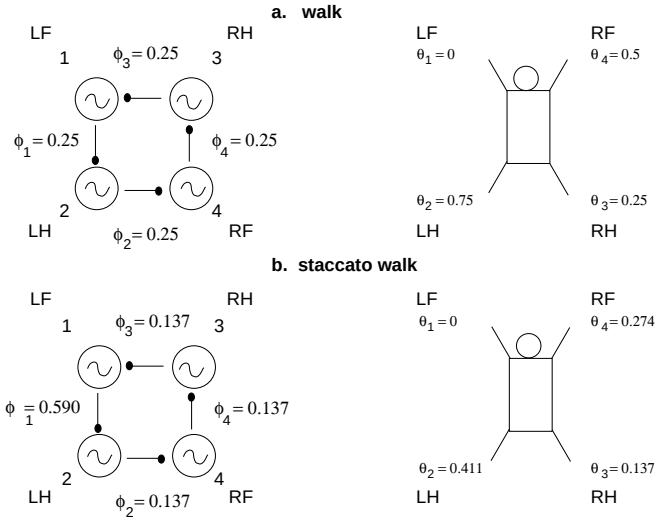

Fig. 7a,b. Illustration of phasic relationships. ϕ_i denotes the fraction of a cycle by which the initiation of the burst in the presynaptic oscillator (the ith oscillator) follows that in its postsynaptic oscillator. Thus, in order to calculate the relative phase difference between an oscillator and the reference oscillator (LF, i = 1), begin at the reference oscillator, then sum the phase differences around the ring in a clockwise direction until the oscillator for which the relative phase is desired is reached. If the sum is not greater than or equal to 0 and less than 1, add an integer in order to renormalize it. **a** In a walk, the phase drop between adjacent oscillators (ϕ_i) is constant at 0.25; therefore the sum around the ring is 1. The relative phases are as follows: $\theta_1 = 0; \theta_2 = \phi_3+\phi_4+\phi_2 = 0.75; \theta_3 = \phi_3 = 0.25; \theta_4 = \phi_3+\phi_4 = 0.5$. **b** In a staccato walk, there are two distinct values of ϕ, one of which is repeated three times; the sum around the ring is 1 as in the walk. The relative phases are as follows: $\theta_1 = 0; \theta_2 = \phi_3 + \phi_4 + \phi_2 = 1.411 = 0.411; \theta_3 = \phi_3 = 0.137; \theta_4 = \phi_3 + \phi_4 = 0.274$. There is a longer pause between burst initiation in oscillator 2 and 1 (0.590 cycle) than between other consecutive burst initiations (0.137 cycle), hence the staccato nature of this mode

Also in Fig. 8a, a staccato gallop was predicted (see the squares) in which three values of ϕ are equal to 0.598 and the fourth is equal to 0.203. This prediction was obtained in a similar fashion to the previous prediction, but in this case $3\phi_i + \phi_j = 2(1 + F(\phi))$ (see Appendix, Special Case II). Again, the observed phasic relationships are in close agreement with the predictions (Table 1). In Fig. 8b, the staccato walk no longer exists due to the flattening of the PRC curve at more depolarized stimulus currents. The staccato gallop remains, but is at the limit of its stability. Table 1 shows that the PRC analysis revealed one negative slope associated with this mode, but of such small magnitude as to be apparently within the error of our methods. We have called this mode a 'gallop' because the relative phases (θ) are within 17% of the nominal phasic relationships in a rotary gallop (Fig. 2). This criterion is similar to that used by others (Collins and Richmond 1994) based on the variability in phasic relationships observed in locomoting quadrupeds. In order to achieve exactly the nominal phasic relationships given by Alexander (1984) for a gallop, three values of ϕ with the same $F(\phi)$ are required (see Sect. 4 and Appendix), rather than just two for the staccato (approximate) gallop. In addition, the walk (diamond), bound (cross), and lateral walk (asterisk) have gained stability since the points at the corresponding values of ϕ now fall in regions of positive slope. In Fig. 8c, further flattening of the PRC eliminated the gallop, leaving only the walk, bound, and lateral walk.

The PRC analysis can predict from the information in the PRCs alone whether a gaitlike pattern will be observed. Therefore, this method can be applied to experimental preparations as well as to mathematical models. The application of PRC methods to mathematical models is computationally less intensive than a random search of the multidimensional state space associated with a circuit model, and also can provide some insight into how the parameters of the model might be adjusted in order to produce a desired pattern. The PRC analysis alone does not indicate how likely it is that a particular pattern will be observed given random initial conditions. Instead, this likelihood was determined by trial and error as in Fig. 4.

The analysis given in the Appendix makes predictions about the behavior of an identically coupled network of four identical oscillators in a ring. Given the mapping of the oscillators in a ring to the legs of a quadruped as shown in Fig. 1, then the existence and stability of certain gaits implies the existence of certain others (see Appendix). For example, the existence of the trot implies the existence (at the same frequency) of the pace, the bound, the pronk, and four other nonphysiological modes in which any three legs are in phase but the fourth is not (we have termed this a 'tripod' mode). The reasoning is straightforward: if a trot exists, then ϕ= 0 and ϕ= 0.5 have the same value of $F(\phi)$. Hence, the bound (ϕ = 0.5) and the pronk (ϕ = 0) exist. The remaining six gaits are produced by pairs of values of ϕ, two equal to 0 and two equal to 0.5. There are six distinct possible ways to assign these values around the ring (see Appendix). There are four possible tripod modes because any of the four legs can be the one that is out of phase. These four modes are an example of rotational symmetry, because they can be produced by having each oscillator take the role of the next one in the ring (a rotation). The gallop is another mode with rotational symmetry: the existence of a transverse gallop implies the existence of a rotary gallop and vice versa. There are two mirror image (with respect to the bilateral symmetry of the quadruped) variants of each type of gallop, depending upon whether the front right foot or the front left foot strikes first in each cycle.

3.4 Use of PRC analysis to design a ring circuit for quadrupedal locomotion

The simulations in the preceeding sections suggest that one way to effect a transition between gaits would be simply to perturb the circuit so that the oscillatory activity is shifted between modes that coexist at a particular parameter setting (Haken et al. 1985; Park et al. 1996), between a walk and a bound at 0 nA stimulus intensity (see Fig. 4c). The work of von Holst (1993) suggests that different oscillatory patterns (modes) of locomotion can coexist in fish: he was able to switch the patterns of coordination between different fins of a fish from in phase to out of phase merely by pinching the fish's tail, which could be interpreted as a perturbation. In horses, data on oxygen consumption versus speed (Hoyt and Taylor 1981) suggest the coexsistence of the trot and the gallop over a range of speed, which is consistent with treadmill experiments using cats that have shown spontaneous switching between these two modes in the intermedi-

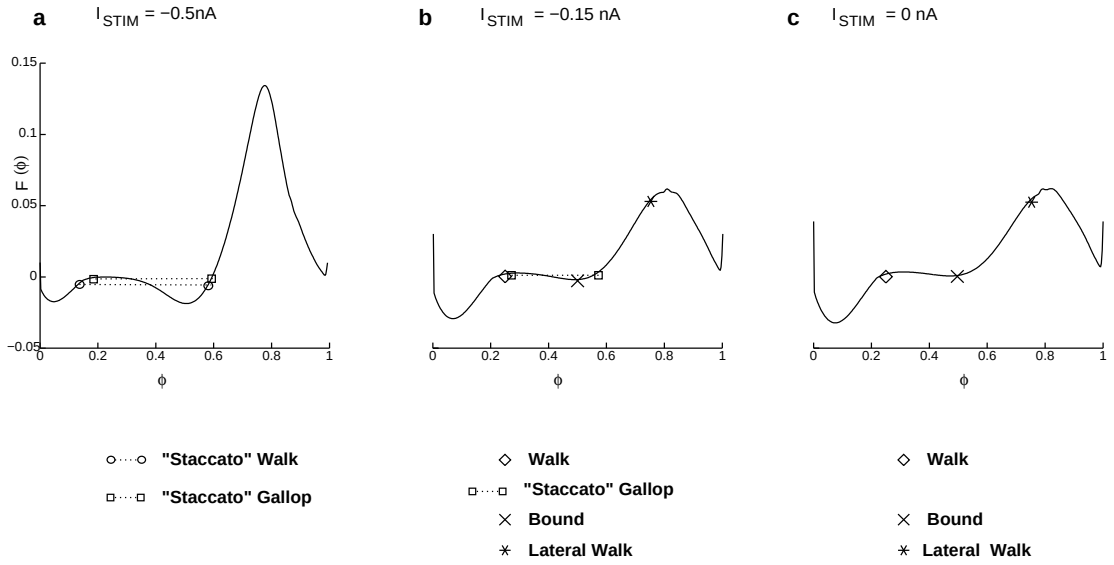

Fig. 8a–c. Phase response curves as I_{STIM} is varied. The PRCs at three different values of I_{STIM} (the same three used in Fig. 4) are shown, and the modes predicted for a ring circuit by the analysis of these curves are summarized at the bottom. The symbols identify predicted stable modes for each curve, except that the staccato gallop (or 'gallop') mode at I_{STIM} = 0 nA is also identified even though the resolution of our method was not good enough to predict the stability of this mode. The *horizontal dashed lines* connect points with identical values of $F(\phi)$

Table 2. Predicted and observed phasic relationships around the ring (ϕ_i) and with respect to the reference oscillator (θ_i)

I_{STIM}	Gait		ϕ_1	ϕ_2	ϕ_3	ϕ_4	P_1(ms)	θ_2	θ_3	θ_4
−0.5	s. walk	predicted	0.590	0.137	0.137	0.137	15966.8	0.411	0.137	0.274
		observed	0.592	0.136	0.136	0.136	15963.6	0.408	0.136	0.272
−0.5	s. gallop	predicted	0.599	0.599	0.599	0.203	16031.2	0.398	0.603	0.795
		observed	0.600	0.600	0.601	0.199	16031.8	0.40	0.601	0.80
−0.15	walk	predicted	0.25	0.25	0.25	0.25	13249.4	0.75	0.25	0.5
		observed	0.25	0.25	0.25	0.25	13249.6	0.75	0.25	0.5
−0.15	'gallop' [a]	predicted	0.567	0.567	0.567	0.300	13255.8	0.434	0.567	0.867
		observed	0.567	0.567	0.568	0.297	13255.6	0.432	0.568	0.865
−0.15	bound	predicted	0.50	0.50	0.50	0.50	13210.7	0.50	0.50	0.0
		observed	0.50	0.50	0.50	0.50	13209.5	0.50	0.50	0.0
−0.15	l. walk	predicted	0.75	0.75	0.75	0.75	13815.8	0.25	0.75	0.50
		observed	0.75	0.75	0.75	0.75	13813.6	0.25	0.75	0.50
0.0	walk	predicted	0.25	0.25	0.25	0.25	12693.2	0.75	0.25	0.5
		observed	0.25	0.25	0.25	0.25	12693.3	0.75	0.25	0.5
0.0	bound	predicted	0.50	0.50	0.50	0.50	12684.6	0.50	0.50	0.0
		observed	0.50	0.50	0.50	0.50	12684.3	0.50	0.50	0.0
0.0	l. walk	predicted	0.75	0.75	0.75	0.75	13235.2	0.25	0.75	0.50
		observed	0.75	0.75	0.75	0.75	13235.7	0.25	0.75	0.50

The ϕ_i were obtained by dividing the ϕ_i in Table 1 by the corresponding $1 + F(\phi)$. The predicted periods (P_1) were obtained by multiplying $(1 + F(\phi))$ by the measured intrinsic period. The intrinsic periods were 12745.3 ms at I_{STIM} = 0 nA, 13285.9 msec at $I_{STIM} = -0.15$ nA and 16050.9 ms at $I_{STIM} = -0.5$ nA. θ_1 is zero by convention in all cases. The remaining θ_i were computed as follows: $\theta_2 = \phi_3 + \phi_4 + \phi_2; \theta_3 = \phi_3; \theta_4 = \phi_3 + \phi_4$. Integers were then added or subtracted to produce a phase between 0 and 1

[a] This mode had one negative slope with a very small magnitude (see text)

ate region between trotting and galloping (Shik et al. 1966). Such an overlap between modes should cause the transition between a trot and a gallop to occur at different speeds depending upon whether the speed is increasing or decreasing; this phenomenon is known as hysteresis. Thus, in this transition region, competing coexisting attractors are justified by the data, but in all other parametric regions, a single attractor corresponding to one gait should dominate.

Transitions between gaits can be achieved in our model by changing the value of the control parameter I_{STIM}. For example, at $I_{STIM} = -0.5$ nA, the model must either be in a staccato walk or in a staccato gallop mode, but since neither of these modes exists at I_{STIM} = 0 nA, if I_{STIM} is changed from −0.5 nA to 0 nA, a transition from the staccato mode to one of the stable modes at 0 nA must occur. While a systematic study was not made, it appeared that a staccato walk transitioned to a walk whereas a staccato gallop transitioned to a bound. These transitions were slow (not shown) due to the weak coupling, as mentioned above. While these are not the transitions observed in a quadruped, the analysis in the preceeding two sections provides a blueprint for a novel design method for a quadrupedal pattern generator that goes from stance to a walk to a trot to a gallop (with hysteresis in the latter transition) as a control parameter (stimulus

intensity) is varied. That is, in order for a ring circuit of oscillators to produce any given pattern in which they are all entrained at the same frequency, the required characteristics of the PRCs can be deduced a priori. A separate issue, not addressed in this study, is how to design an oscillator that will produce the appropriate PRC.

Figure 9 shows a freehand drawing of the hypothetical PRCs for a ring circuit that produced the correct gait transitions as stimulus intensity is increased. Initially, only a walk gait is stable as indicated by the diamond in Fig. 9a. A PRC with a single minimum and maximum also has a single region of positive slope, and therefore cannot have two or more values of ϕ with the same value of $F(\phi)$ that both have positive $F'(\phi)$. Therefore the only possible gait modes associated with this PRC are those with four equal values of ϕ. Of the four possible such modes (see Appendix, Special Case I), only the walk (ϕ = 0.25) is stable since it alone falls in the region of positive slope. As the stimulus intensity is increased (equivalent to making I_{STIM} more depolarized in our model), another local minimum and maximum appear near ϕ = 0.25, and the walk becomes unstable since it falls in the negative slope region created by the new minimum and maximum. The second region of positive slope enables a new mode composed of pairs of values of ϕ near 0.25 (0.24 and 0.26 for example) that is associated with a stable trot-like walk. This mode becomes more like a trot as the new minimum and maximum move farther away from each other, until in Fig. 9c the gait is much closer to a trot than a walk. This simulates the actual transition between a walk and a trot in quadrupeds, which is gradual (Shik and Orlovsky 1976). Then in Fig. 9d, a third maximum-minimum pair appears near 0.5, so that 0.5 falls in the negative slope region and a bound is unstable. This third region of positive slope enables a new mode (with three ϕ_i equal to 0.55 and one equal to 0.35) to coexist with the trot. The new mode produces a 'staccato' gallop with phasic relationships very close to those published for a gallop. A 'true' gallop with three distinct values of ϕ would require yet another maximum-minimum pair to be created, so it is plausible that the gallop, whose phasing is somewhat arbitrary, may actually correspond to what we have called a staccato gallop. Finally, in Fig. 9e, the trot ceases to exist as the hump in the PRC responsible for it is flattened out by increasing stimulus intensity.

We have focused here on the gait transitions exhibited by cats and horses. Other quadrupeds have differing sequences of gait transitions (Hildebrand 1976, 1977). However, if a ring circuit can indeed capture the essential dynamics of the CPG for quadrupedal locomotion, then perhaps the adaptive influence of evolution, operating within the constraints imposed upon a particular species by its flexibility and requirement for mechanical stability (balance), can produce species-specific PRCs for the limb oscillators, resulting in the differing gaits characteristic of different quadrupeds. Along these lines, the walk sequence is the single one that maximizes static stability (McGhee and Frank 1968); hence it is ubiquitous among quadrupeds.

3.5 Additional modes observed due to bistability

As described in Sect. 1, the individual oscillators that we have employed have a bistable range from about I_{STIM} = 0.2 to I_{STIM} = 1.8 nA (Butera et al. 1996). In this bistable range, a depolarized mode corresponding to tonic firing, or beating, coexists with an oscillation corresponding to bursting activity. Therefore, when the neurons are coupled into a four-element circuit, one might expect to observe modes corresponding to all 16 possible combinations of beating and bursting neurons. We have indeed observed all 16 possible combinations. However, in the circuit, all modes in which fewer than four oscillators exhibited a full-scale oscillation corresponding to bursting were observed at values of I_{STIM} that were slightly higher than 1.8 nA, the upper limit of the bistable range in an individual oscillator. For values of I_{STIM} greater than 1.8 nA, PRC analysis is impossible, because the uncoupled circuit elements no longer oscillate. Although all 16 binary combinations referred to above have been found, the full complement has not been shown to coexist at a single value of I_{STIM}.

Some of these combinations are shown in Fig. 10. In fact, there are more than 16 possible combinations since modes with the same number of bursters and beaters may also be distinguished by phasic relationships. For example, in Fig. 10a and b, all four oscillators are in a bursting mode, but Fig. 10a represents a bound and Fig. 10b represents a walk. In Fig. 10c, there are two bursters (LH, RH) while the other two are beaters, albeit with a slight oscillation in frequency, since the spike frequency is always above zero. Thus, a ring circuit composed of bistable elements can produce patterns in which only some of the oscillators are active, with no change in connectivity. Thus, in principle, an analogous locomotor CPG could produce behaviors in addition to quadrupedal locomotion, such as hopping on the hind legs, as suggested by Fig. 10c. In Fig. 10d, there are three bursters and one beater, whereas in Fig. 10e, potentially corresponding to a scratch, there is one burster and three beaters. Finally, in Fig. 10f all oscillators exhibit a low-amplitude oscillation corresponding to four tonically spiking neurons, perhaps corresponding to a rigid stance. Hence, bistability endows these neurons with a type of complexity that is not amenable to PRC analysis. Figure 10 does not provide a complete listing of all modes that were detected in the parametric region just above the threshold for oscillatory activity in a single circuit element. For example, another mode that has been detected (not shown) at I_{STIM} = 1.9 nA has a 3 to 1 entrainment ratio between the frequency of the front legs and the hind legs. The frequency of occurrence of the mode corresponding to four beaters (Fig. 10f) in random state-space searches (described above) steadily increases from a couple of percent at I_{STIM} = 1.9 nA to over 50% at 2.2 nA. The bound, on the other hand (Fig. 10a), predominates at 1.9 nA, but was not found at 2.0 nA and reappeared at 2.1 nA. Due to the capacity of the circuit to exist in one of numerous modes based on the history of the activity of the circuit, these modes endow this circuit with the potential for use in an entirely different context, as an associative memory.

At sufficiently depolarized values of I_{STIM} (2.5 nA), most initial conditions resulted in a nonoscillatory depolar-

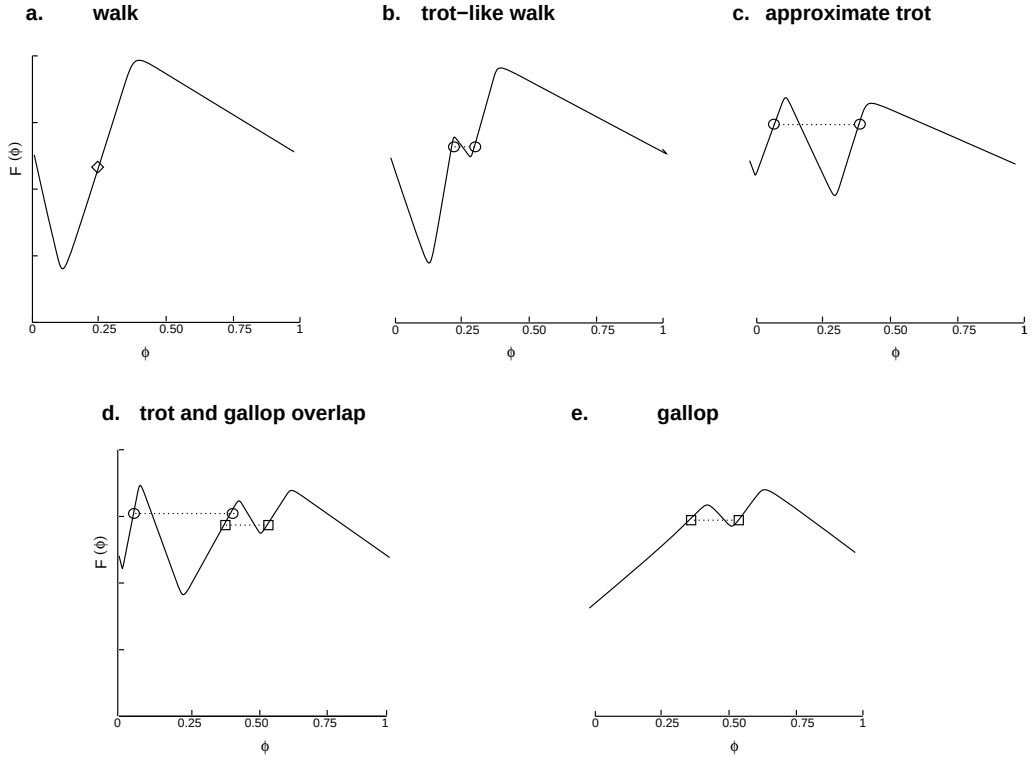

Fig. 9a–e. Idealized PRC for Gait Transitions. The shape of the PRC must change with increasing stimulus intensity in order for a ring circuit composed of oscillators characterized by these PRCs to reproduce the gait transitions exhibited by quadrupeds. The curves were not generated by simulations but are idealized schematics. **a** The *diamond* represents a stable walking mode. **b** The *circles* represent the two values of ϕ that comprise a stable trot-like walk mode that is very close to a walk. **c** The *circles* show the values of ϕ for a trot-like walk that is nominally a trot. **d** The *circles* still represent the values of ϕ for a trot-like walk, and the *squares* represent the two values of ϕ in a stable staccato gallop that has phasic relationships close to the nominal values for a gallop. **e** The *squares* indicate that only the nominal gallop mode exists and is stable for this PRC. The *horizontal dashed lines* connect points with identical values of $F(\phi)$

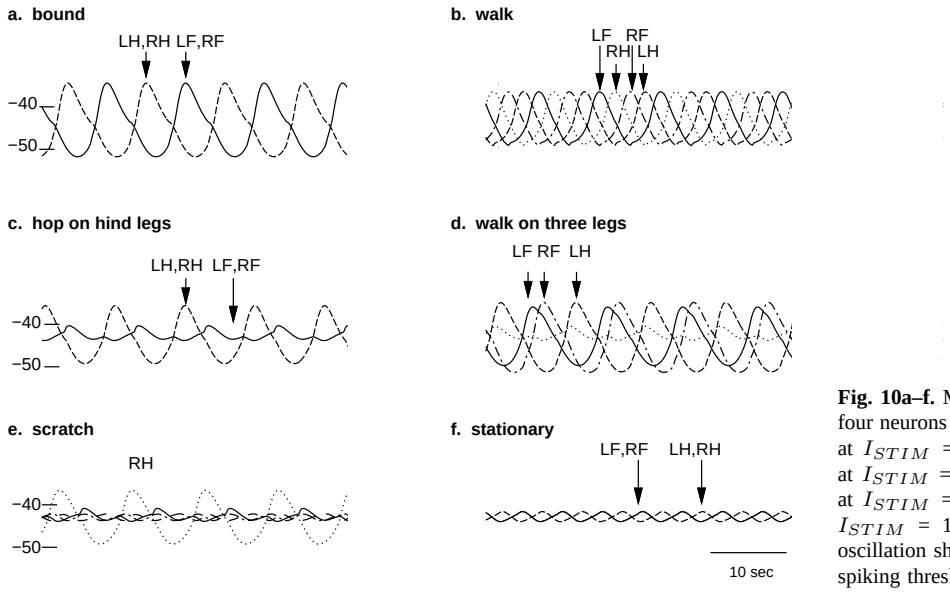

Fig. 10a–f. Modes with subsets of bursters. In **a** and **b** all four neurons are bursters; these simulations were generated at I_{STIM} = 1.9 nA. In **c** there are two bursters, shown at I_{STIM} = 2.0 nA. In **d** there are three bursters, shown at I_{STIM} = 2.0 nA. In **e** there is one burster, shown at I_{STIM} = 1.9 nA. In **f**, there are no bursters; the small oscillation shown at I_{STIM} = 2.0 nA is always above the spiking threshold

ized state (not shown). However, in some instances a curious double-period lateral walk mode was observed (not shown). The inhibition produced by a burst was sufficient to annihilate the subsequent burst in the postsynaptic neuron, hence the double period.

4 Discussion

4.1 Comparison with other models of gait generation

Schoner et al. (1990) modeled gait generation using variables representing the three relative phases resulting from setting the right front foot as a constant reference point. The rates of

change of the relative phases for each leg are described by periodic functions of the phase differential between that leg and each of the two adjacent legs. The functions are represented as second-order Fourier series, and the Fourier coefficients are the coupling parameters of the model. Hence, it is difficult to interpret this model physiologically, but Schoner et al. obtained gait-like patterns. They observed two types of transitions as they varied the coupling parameters of their model: continuous, such as between a walk and a trot, and abrupt with hysteresis, such as between a trot and a bound. Interestingly, their approach, like ours, predicts a parametric region in which the pronk (they call it the jump), bound (gallop), trot, pace, and the four tripod modes are all stable. While in this study, the coupling parameters were the bifurcation, or control, parameters, one of the authors (Kelso 1995) has suggested that frequency could also be a control parameter. He further theorized that gait transitions are nonequilibrium phase transitions, which is another way of phrasing our hypothesis regarding gait transitions.

Using a model of coupled nonlinear oscillators, Stafford and Barnwell (1985) also achieved gait transitions by changing the interlimb coupling terms. Each leg was represented by four state variables, one each for the hip, knee, ankle, and toe flexors (the oscillatory pattern was assumed to be generated by flexor, not extensor, activity), and the interlimb coupling included components for selective coupling between the 16 flexor groups. For example, their model produced a walk when the mutual interlimb coupling terms between all four legs were sufficiently strong and equal (tetrahedral symmetry, see Fig. 11a). When the diagonal contralateral inhibition was reduced (see Fig. 11b), a trot was produced. Finally, when the diagonal contralateral inhibition was restored and the homologous contralateral inhibition removed (see Fig. 11c), a bound was produced (they call it a gallop). This final configuration is qualitatively equivalent to the ring that we used, except for the bidirectional coupling. There are three ways to map a ring circuit onto the legs of a quadruped (Fig. 11b–d), but, as we stated in Sect. 1, only the circuit in Fig. 11c produces the sequence of footfalls observed in a walk. In our simulations of our ring model (unpublished observations) using a tetrahedrally symmetric configuration, a walk sequence, in which each leg was 90° out of phase with the next leg, was produced as in their model. However, the walk sequence coexisted with five other patterns that were equally likely to result from random initial conditions and corresponded to the other five possible leg sequences, exemplified by the lateral walk and the four gallops. Thus, although Stafford and Barnwell do not mention whether they found other patterns in their model coexisting with the walk, our results suggest that they exist. Nonetheless, they show clearly that rewiring the interlimb circuit in a physiologically interpretable way is a viable method of changing gaits, albeit not the only possible one.

Yuasa and Ito (1990) produced a method for designing a gait pattern generator using four simple oscillators with nonidentical coupling. In their approach, as in that of the two previously discussed studies, the patterns of interlimb connection were varied in order to produce simulated gait transitions. The uncoupled two-variable oscillators that they used were designed to relax to a circular limit cycle with a constant angular velocity, with a state variable representing

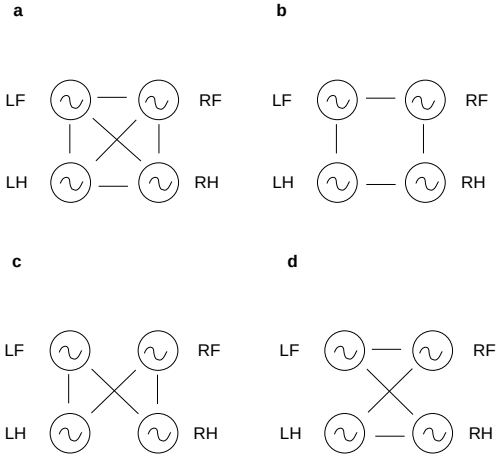

Fig. 11a–d. Four different interlimb connection schemes. The scheme in **a** does not map onto a ring but rather has tetrahedral symmetry. The schemes in **b**, **c**, and **d** represent a ring circuit with all possible mappings to the legs of a quadruped

the phase of the oscillator and one representing the radial distance from the origin. The functional dependence of the phase of each oscillator on the phases of the other oscillators was adjusted to achieve the desired phasic relationships in a gait. The precise form of the couplings was determined by minimizing an appropriate potential function in phase space, so, as in Schoner et al. (1990), there is no clear physiological interpretation of their model.

Collins and Richmond (1994) have taken a different and novel approach that inspired our own study. In their model, which used the same ring configuration that we have used, the interlimb coupling was fixed. They employed three identically connected circuits, which differed in the type of simple nonlinear oscillators (Van der Pol, Fitzhugh-Nagumo, or Stein) that comprised the circuit elements. Rather than varying the connections, they added a driving function for each oscillator and varied the parameters of the driving function. This function was slightly different for each of the three types of simple nonlinear oscillators that they studied but always had a constant component and a sinusoidal component. The magnitude of both components and the frequency of the sinusoidal input were varied, along with one control parameter that affected the characteristic amplitude and/or frequency of the oscillator. For each of the three circuits, they found a set of parameters at which a pattern corresponding to a walk was generated. Then, by increasing the values of up to four independent parameters, a transition to a trot, and then to a bound was obtained. In our recreation[4] of their simulations at the nominal parameter values they gave for each gait, we found coexisting attractors in every case. Collins and Richmond alluded to the presence of these competing attractors. We found that the bound was stable at each of the nominal sets of parameters, and predominated in all cases except at the parameter settings given for the walk using the Stein oscillators; in that case, the walk attracted about the same number of random initial conditions as the

[4] There were two typographical errors in the Collins and Richmond paper regarding the FitzHugh-Nagumo model: the parameter values given for k_1 and k_2 were interchanged, and the second plus sign in the equation for $\dot{x}_i$ should have been a minus.

bound. In accordance with the predictions in the Appendix, the pace coexisted with the trot whenever the trot occurred, and in the Van der Pol and Stein circuits the four variants of the tripod gait were also detected. We did not detect the tripod gait in the FitzHugh-Nagumo model, perhaps as a consequence of the fact that we detected the trot and the pace themselves very infrequently (combined, they attracted less than 6% of the random initial conditions). In the trot observed by Collins and Richmond, the diagonal legs were not exactly in phase: this condition would result if the values of the pairs of ϕ_i were not exactly equal to 0 and 0.5, but only approximate (per the Appendix, the two distinct values must add up to 0.5).

4.2 The ring circuit as a model for quadrupedal locomotion

It has been suggested that successive bifurcations leading to gait transitions break more and more symmetry (Collins and Stewart 1993) we propose that, in a ring model of gait generation, successive bifurcations correspond to a change in the number of distinct values of ϕ required to satisfy the criteria for stable gait generation described in Sect. 3. Whether the transition is gradual, as in a walk-trot transition, or abrupt with hysteresis, as in the trot-gallop transition, depends upon how the lower-speed gait loses its stability. The PRC analysis shows why some gaits are more likely to be observed in a ring model than others: the simplest require only one value ϕ that satifies the three criteria described in Sect. 3, such as the walk and bound. Others, such as the pace and trot, require two, assuming the mapping of homologous contralateral legs to nonadjacent oscillators, still others such as the gallops may require three (discussed below), and a canter (see Appendix, Special Case IV) requires four. As discussed above, previous, presumably simpler models did not generate a gallop, and required a phasic input or rewiring to generate a trot. The increased complexity of component neuronal elements naturally leads to a more complex PRC with more peaks and valleys, thus creating the potential for some of the modes requiring multiple ϕ values to exist – hence the utility of more complex neuronal oscillators in models of pattern generation. For example, if the dependence of s and c on q (see Sect. 2) in our model is turned off, the PRC becomes less complex, and the circuit is less likely to exhibit the galloping mode.

There are two potential mappings of the legs onto the oscillators of the ring, besides the one that we have chosen. In one, where diagonal contralateral legs are not adjacent in the ring (like Fig. 11b, but with unidirectional coupling), a rotary gallop sequence replaces the walk and the trot changes places with the bound. In the other, in which ipsilateral legs are mapped to nonadjacent oscillators (like Fig. 11d), a transverse gallop sequence replaces the walk and the pace and the bound exchange places. We chose the mapping that produces the walk since it is the only one of the three that produces the correct sequence for the oscillatory mode with a relative phase of 0.25 between successive legs. The effect of unidirectional versus bidirectional coupling is to break the symmetry between gaits that correspond to an opposite sense of rotation around the ring, such as the walk and the lateral walk in the scheme that we have chosen.

Some quadrupeds show a preference for a trot over a pace (or for a transverse versus a rotary gallop), whereas our ring model predicts that a pace would always coexist with a trot (see Appendix, Special Case IIIa), and as rotational variants, neither would be statistically preferred (the same holds for the gallops). One explanation for these discrepancies is that in a real quadruped, a deviation from identical oscillators or identical coupling could break the symmetry of the ring sufficiently to favor one of what would otherwise be equivalent rotational variants. The shape of the PRC curve is somewhat sensitive to the magnitude and kinetics of the synaptic coupling, but varying the delay times between oscillators may be a simpler and more effective way to break the symmetry since adding a delay predictably shifts the PRC curve right or left by the magnitude of the delay. For example, if the delay times in the diagonal contralateral pathways were slightly different from those of the ipsilateral path, it might be sufficient to bias the system to favor a trot or a pace, without losing the walk and gallop at other stimulus intensities. Slightly nonidentical oscillators could work as well.

Clearly, the ring circuit is a simplification of the spinal pattern generator for quadruped gait generation. For example, it does not include coupling between homologous contralateral legs. If our hypothesis that gait transitions are an emergent property of the nonlinear dynamics of the system is correct, a low-order model such as ours may nonetheless capture certain essential aspects of the physiological circuit. Stein (1976) has suggested that the mathematics of coupled oscillators, and the PRC in particular, should be utilized in the design and analysis of interlimb coordination. Our analysis predicts the PRC required at different levels of stimulus intensity for a ring circuit design for the control of quadrupedal locomotion. If a preparation could be developed in which the spinal cord oscillators associated with each limb could be studied in isolation so that a PRC could be generated, the predictions in Fig. 9 could be tested. In addition, perhaps the design method we have suggested could be applied and tested in legged robots.

Acknowledgements. We would like to thank Dr. Paul Smolen for his comments on an earlier draft of the manuscript. This work was supported in part by Office of Naval Research Grant N00014-95-1-0579 and National Institute of Mental Health Award K05 MH00649. R.J.B. was supported by a Whitaker Foundation Graduate Fellowship in Biomedical Engineering.

Appendix

Definitions: $\phi_1 = \theta_1 - \theta_2$; $\phi_2 = \theta_2 - \theta_4$; $\phi_3 = \theta_3 - \theta_1$; $\phi_4 = \theta_4 - \theta_3$; θ_i indicates the phase of an oscillator relative to θ_1 (but any other reference would work as well). An asterisk indicates that there are rotational variants. The phasic relationships for only one of four variants is shown.

General case: $\phi_1 + \phi_2 + \phi_3 + \phi_4 = n$, where $n \in (0, 3)$

Special case I: $\phi_1 = \phi_2 = \phi_3 = \phi_4 = \phi_i$

pronk $\phi_i = 0.00$, $n = 0$	$\theta_1 = 0.00$; $\theta_2 = 0.00$; $\theta_3 = 0.00$; $\theta_4 = 0.00$
transverse walk $\phi_i = 0.25$, $n = 1$	$\theta_1 = 0.00$; $\theta_2 = 0.75$; $\theta_3 = 0.25$; $\theta_4 = 0.50$
bound $\phi_i = 0.5$, $n = 2$	$\theta_1 = 0.00$; $\theta_2 = 0.50$; $\theta_3 = 0.50$; $\theta_4 = 0.00$
lateral walk $\phi_i = 0.75$, $n = 3$	$\theta_1 = 0.00$; $\theta_2 = 0.25$; $\theta_3 = 0.75$; $\theta_4 = 0.50$

Special case II: $\phi_i \neq \phi_j$, $\phi_i = \phi_k = \phi_l$

staccato t. walk*	$3\phi_i + \phi_j = 1$ $0 < \phi_j < \frac{1}{3}$	$\theta_1 = 0; \theta_2 = -\phi_i; \theta_3 = \phi_i; \theta_4 = \phi_i + \phi_j$
staccato gallop*	$3\phi_i + \phi_j = 2$ $\frac{1}{3} < \phi_j < \frac{2}{3}$	$\theta_1 = 0; \theta_2 = -\phi_i; \theta_3 = \phi_i; \theta_4 = \phi_i + \phi_j$
staccato l. walk*	$3\phi_i + \phi_j = 3$ $\frac{2}{3} < \phi_j < 1$	$\theta_1 = 0; \theta_2 = -\phi_i; \theta_3 = \phi_i; \theta_4 = \phi_i + \phi_j$
transitional*	$\phi_i = \frac{1}{3}, \phi_j = 0$	$\theta_1 = 0; \theta_2 = \frac{2}{3}; \theta_3 = \frac{1}{3}; \theta_4 = \frac{1}{3}$
	$\phi_i = \frac{2}{3}, \phi_j = 0$	$\theta_1 = 0; \theta_2 = \frac{1}{3}; \theta_3 = \frac{2}{3}; \theta_4 = \frac{2}{3}$

Note: In-phase oscillators are adjacent in the ring.

Special case III: $\phi_i + \phi_j = \frac{n}{2}$, $\phi_k + \phi_l = \frac{m}{2}$, $\frac{m+n}{2} \in [0, 3]$

Special case IIIa: $\phi_i + \phi_j = 0$, $\phi_k + \phi_l = 1$, $\phi_i = \phi_j = 0$, $\phi_k = \phi_l = 0.5$

trot	$\phi_1 = \phi_4 = 0.5, \phi_2 = \phi_3 = 0$	$\theta_1 = 0; \theta_2 = 0.5; \theta_3 = 0; \theta_4 = 0.5$
pace	$\phi_1 = \phi_4 = 0, \phi_2 = \phi_3 = 0.5$	$\theta_1 = 0; \theta_2 = 0; \theta_3 = 0.5; \theta_4 = 0.5$
tripod*	$\phi_1 = \phi_3, \phi_2 = \phi_4$ or $\phi_1 = \phi_2, \phi_3 = \phi_4$	$\theta_1 = 0; \theta_2 = 0; \theta_3 = 0; \theta_4 = 0.5$

Note: If any of the above modes exist, that implies the existence of the other two, as well as the pronk and the bound.

Special case IIIb: $\phi_i + \phi_j = 1, \phi_k + \phi_l = 1, \phi_i = \phi_j = 0.5, \phi_k \neq \phi_l$ (observed $\phi_k \approx 0.4$)

gallop*	$\phi_2 = \phi_3$ or $\phi_1 = \phi_4$	$\theta_1 = 0; \theta_2 = -\phi_1; \theta_3 = 0.5; \theta_4 = 0.5 - \phi_1$
half-bound*	$\phi_1 = \phi_3$ or $\phi_2 = \phi_4$ *or* $\phi_1 = \phi_2$ or $\phi_3 = \phi_4$	$\theta_1 = 0; \theta_2 = 0.5; \theta_3 = \phi_3; \theta_4 = 0$

Note: If either of the above modes exist, that implies the existence of the other, as well as the bound.

Special case IIIc: $\phi_i + \phi_j = 1, \phi_k + \phi_l = 1, \phi_i = \phi_j, \phi_k = \phi_l$

assymetric bound*	$\phi_1 = \phi_3$ or $\phi_1 = \phi_4$	$\theta_1 = 0; \theta_2 = \phi_i; \theta_3 = \phi_i; \theta_4 = 0$
assymetric half-bound*	$\phi_1 = \phi_2$	$\theta_1 = 0; \theta_2 = \phi_i; \theta_3 = \phi_i; \theta_4 = 2\phi_i$

Note: If either of the above modes exist, that implies the existence of the other.

Special case IV: $\phi_i + \phi_j + \phi_k + \phi_l = 1$, $\phi_i \neq \phi_j \neq \phi_k \neq \phi_l$

canter	$\phi_1 = 0.2$, $\phi_2 = 0$, $\phi_3 = 0.5$, $\phi_4 = 0.3$	$\theta_1 = 0$; $\theta_2 = 0.8$; $\theta_3 = 0.5$; $\theta_4 = 0.8$

References

Alexander RM (1984) The gaits of bipedal and quadrupedal animals. Int J Robot Res 3:49–59

Butera R Jr, Clark JW, Byrne JH (1996) Dissection and reduction of a modeled bursting neuron. J Comp Neurosci 3:199–223

Collins J (1995) Gait transitions. In: Arbib MA, (ed), The Handbook of Brain Theory and Neural Networks. MIT Press, Cambridge, Mass, pp 420–423

Collins JJ, Richmond SA (1994) Hard-wired central pattern generators for quadrupedal locomotion. Biol Cybern 71:371–385

Collins JJ, Stewart IN (1993) Coupled nonlinear oscillators and the symmetries of animal gaits. J Nonlinear Sci 3:349–392

Collins JJ, Stewart I (1994) A group-theoretic approach to rings of coupled biological oscillators. Biol Cybern 71:95–103

Demir SS, Butera RJ, De Franceshi AA, Clark JW, Byrne JH (1997) Phase sensitivity and entrainment in a modeled bursting neuron. Biophysical J 72:579–594

Gambaryan P (1974) How mammals run: anatomical adaptations. Wiley, New York

Glass L, Mackey M (1988) From clocks to chaos: the rhythms of life. Princeton University Press, Princeton, NJ

Goldbeter A (1996) Biochemical oscillations and cellular rhythms. Cambridge University Press, Cambridge

Grillner S (1975) Locomotion in vertebrates: central mechanisms and reflex interaction. Physiol Rev 55:247–306

Guckenheimer J, Holmes P (1983) Nonlinear oscillations, dynamical systems, and bifurcation of vector fields. Springer, Berlin Heidelberg New York

Hairer E, Wanner G (1991) Solving ordinary differential equations. II. Stiff and differential-algebraic problems. (Springer series in computational mathematics). Springer, Berlin Heidelberg New York

Haken H, Kelso JA, Bunz H (1985) Theoretical model of phase transitions in human hand movements. Biol Cybern 51:347–356

Halbertsma JM, Miller S, van der Meche FG (1976) Basic programs for the phasing of flexion and extension movements of the limbs during locomotion. In: Herman R, Grillner S, Stein P, Stuart D (eds) Neural control of locomotion. (Advances in behavioral biology, vol 18) Plenum Press, New York, pp 489–517

Hildebrand M (1976) Analysis of tetrapod gaits: general considerations and symmetrical gaits. In: Herman RM, Grillner S, Stein PSG, Stuart D (eds), Neural control of locomotion. (Advances in behavioral biology, vol 18) Plenum Press, New York, pp 203–236

Hildebrand M (1977) Analysis of asymmetrical gaits. J Mammal 58:131–157

Holst E von (1973) The behavioral physiology of animals and man: the collected papers of Erich von Holst (trans R Martin). University of Miami Press, Coral Gables

Hoyt DF, Taylor RC (1981) Gait and the energetics of locomotion in horses. Nature 292:239–240

Kelso JAS (1995) Dynamic patterns: the self-organization of brain and behavior. MIT Press, Cambridge, Mass

Kopell N (1988) Towards a theory of modelling central pattern generators. In: Cohen AH, Rossignol S, Grillner S (eds) Neural control of rhythmic movements in vertebrates. Wiley, New York, pp 369–413

McGhee RB, Frank AA (1968) On the stability properties of quadruped creeping gaits. Math Biosci 3:331–351

Moore GP, Perkel DH, Segundo JP (1963) Stability patterns in interneuronal pacemaker regulation. In: Paul A (ed). Proceedings of the San Diego symposium for biomedical engineering. La Jolla, Calif, pp 184–193

Murray JD (1989) Mathematical biology. Springer, Berlin Heidelber New York

Park SH, Han SK, Kim S, Ryu CS, Kim S, Yim T (1996) Switching among alternate synchronization patterns in an electrically coupled neuronal model. ETRI J 18:161–170

Pavlidis T (1973) Biological oscillators: their mathematical analysis. Academic Press, New York

Perkel DH, Schulman JH, Bullock TH, Moore GP, Segundo JP (1964) Pacemaker neurons: effects of regularly spaced synaptic input. Science 145:61–63

Schoner G, Jiang WY, Kelso JAS (1990) A synergetic theory of quadrupedal gaits and gait transitions. J Theor Biol 142:359–391

Shik ML, Orlovsky GN (1965) Co-ordination of the limbs during running of the dog. Biophysics 10:1148–1159

Shik ML, Orlovsky GN (1976) Neurophysiology of locomotor automatism. Physiol Rev 56:465–501

Shik ML, Severin FV, Orlovsky GN (1966) Control of walking and running by means of electrical stimulation of the mid-brain. Biophysics 11:756–765

Stafford FS, Barnwell GM (1985) Mathematical models of central pattern generators in locomotion. J Mot Behav 17:61–76

Stein PSG (1976) Mechanisms of interlimb phase control. In: Herman RM, Grillner S, Stein PSG, Stuart DG (eds) Neural control of locomotion. (Advances in behavioral biology, vol18) Plenum Press, New York, pp 465–487

Winfree AT (1980) The geometry of biological time. Springer Berlin Heidelberg New York

Yuasa H, Ito M (1990) Coordination of many oscillators and generation of locomotory patterns. Biol Cybern 63:177–184